Hirshfeld surfaces as approximations to interatomic surfaces

A. Martín Pendás, V. Luaña, L. Pueyo, E. Francisco, and P. Mori-Sánchez
Departamento de Química Física y Analítica, Facultad de Química, Universidad de Oviedo, E-33006-Oviedo, Spain

(Received 18 February 2002; accepted 16 April 2002)

A simple algebraic model is used to show that Hirshfeld surfaces in condensed phases may be understood as approximations to the interatomic surfaces of the theory of atoms in molecules. The conditions under which this similarity is valid are explored, and both kinds of surfaces are calculated in the LiF and CS_2 crystals to illustrate the main results. The link between Hirshfeld and interatomic surfaces provides a physical ground to understand the usage of the former to visualize intermolecular interactions. © *2002 American Institute of Physics.* [DOI: 10.1063/1.1483851]

I. INTRODUCTION

The basic tenet of the atomic and molecular theory is the existence of individual entities, i.e., atoms or molecules, that comprise ordinary matter. These entities exist in real space, and it is legitimate to question about their size and shape. However, quantum state vectors entangle the coordinates of all the particles of a system, making it difficult to isolate atoms within molecules or molecules within molecular aggregates. In spite of these theoretical concerns, molecular surfaces (MS) are becoming increasingly popular and useful.[1] Two main streams are currently used to construct them. The first one uses overlapping atomic spheres of appropriate sizes (often van der Waals radii) to build a suitable volumetric representation of a molecule. The original Corey–Pauling–Koltun (CPK)[2] surfaces lie in this category, but have been superseded by the concept of solvent accessible surfaces.[3] The second one is based on recognizing that a molecule is chemically characterized by its electronic distribution. In these models, it is some functional of the electron density, $\rho(\vec{r})$, that defines the MS. It was long ago recognized[4] that the $\rho \simeq 0.002$ a.u. isosurfaces were strikingly similar to the CPK surfaces. The experimental accessibility of accurate electron densities through modern x-ray diffraction techniques,[5] together with the recent advances in linear scaling methods for the solution of the electronic structure problem[6] are providing the raw data to probe the actual usefulness of the molecular surface concept.

A rather large number of presently active research fields benefit from the quick computation and virtual manipulation of one or another flavor of molecular surfaces:[7] crystal prediction and crystal engineering, solute–solvent interactions, protein folding, protein docking, structure-based drug design, etc. In all these disciplines, intermolecular surfaces are mainly used as powerful tools in the prediction and control of molecular interactions.

The definition of molecular surfaces for interacting molecules leads us back to the problem of partitioning the physical space into atomic or molecular regions. This is a historical problem in solid state physics, and a first approximation to it was presented by Wigner and Seitz in 1933.[8] Wigner–Seitz cells in monoatomic solids are nothing but the Voronoi or proximity polyhedra (PP).[9] A PP contains just one nucleus, displays the full point-group symmetry of its nuclear site, and shares faces with its neighboring PPs. Also, the complete set of PPs of a crystal fill the space without overlapping. However, their generalization to lattices containing more than one atomic species is not easy, needing at least from the specification of the relative sizes of the constituents. The resulting atomic polyhedra are known as weighted proximity polyhedra (WPP) or generalized Wigner–Seitz cells, and have been proposed and used several times in the literature.[10,11] WPPs fill the space, but lack a single and uniform definition.

One of the most firmly rooted answers to this long-standing problem arrived with the concept of interatomic surface (IAS), extracted directly from the theory of atoms in molecules (AIM) developed by Bader and co-workers.[12] Recently, Spackman and Byrom[13] have introduced a method to partition electron densities into fragment contributions based on the Hirshfeld stockholder partitioning scheme.[14] The resulting surfaces have been called Hirshfeld surfaces (HS). Subsequent papers[15,16] have shown that HSs may be reliably used to visualize intermolecular interactions, and that their curvature is somehow related to the nature of those interactions. These observed properties of HSs have contributed to increase their popularity, but their origin and physical justification are still unknown. As Spackman and Byrom showed in the urea crystal, the similarity between the HSs and the IASs is striking, and they ascribed this similarity to the assumption that IASs must coincide with the valleys of the electron distribution in any plane. However, this is not true, and large differences with respect to the valley condition are found in many IASs (see, for instance, the shapes of IASs in Refs. 17 and 18).

In this work we analyze the relation between the HSs and the molecular envelope of the IASs (the atoms in molecules molecular surface, AIMMS) and show that the link actually exists. A simple model of the electron density in a diatomic molecule is used to discuss analytically the geometry of the HSs and to show the close relationship between HSs and IASs in the region of the bond critical point (bcp) (first order saddle of the electron density). Our algebraic arguments are illustrated with the comparison of the HSs and

the AIMMSs in the rock-salt phase of the LiF crystal and the C*mca* phase of the CS_2 crystal. The quantitative comparisons confirm the high performance of the HSs as an approximation to the AIMMSs. This relationship should put the HSs in an interesting computational position: easy to compute and manipulate on the one hand, and clearly related to intermolecular interactions through the AIM connection on the other hand.

The rest of the paper is organized as follows: The next section gives a brief introduction to IASs and HSs. In Sec. III we develop the analytical exponential model to describe the electron density, and apply it to the characterization of HSs and AIMMSs. Finally, in Sec. IV we present two numerical examples that confirm our algebraic predictions. We also summarize our main conclusions.

II. INTERATOMIC SURFACES AND HIRSHFELD SURFACES

The AIM theory is a rigorous formulation of the quantum mechanics of subsystems. It is firmly rooted in one of the more general formulations of quantum mechanics: Schwinger's stationary action principle.[19] The theory shows that a quantum system may be partitioned into subsystems that follow the general quantum laws. These subsystems are uniquely defined in the physical space, contribute additively to all the observables in the system, are quantitatively transferable among families of compounds, and usually contain only one nucleus. Different subsystems are separated by well-defined interatomic surfaces, whose characterization actually defines the subsystems: The IASs are locally zero-flux surfaces of the gradient field of the electron density,

$$\vec{\nabla}\rho(\vec{r})\cdot\vec{n}(\vec{r})=0, \tag{1}$$

where $\vec{n}$ is a unitary normal vector to the surface. Since its initial successes, the AIM theory has come to a mature state as a density-based theory of chemical bonding. It is widely used in molecular chemical physics, and it is starting to provide interesting insights in solids, both with theoretically computed densities[11,17,18,20,21] and, more recently, with experimental ones.[5] Very briefly, if we understand $\vec{\nabla}\rho$ as a vector field, a given IAS may also be viewed as the geometrical locus of all points whose field lines end up at a given bond critical point. Thus an IAS is uniquely associated to a bond path and to a pair of bonded atoms. Being a two-dimensional manifold, we may call it a face. When such a face does not extend to infinity, in its one-dimensional boundary we find (save exceptions) a certain number of ring critical points (second order saddles) and cage critical points (minima of the density). The union of the field lines that start at those cage points and end at the ring points form the boundary of the face. Rings are then edges of the face, while cages may be identified with vertices of it. We have a homeomorphism between an IAS and a polygonal face.

The exterior envelope formed by the juxtaposition of all the IASs of the quantum atoms forming a molecule is the AIM molecular surface (AIMMS). These surfaces are closed in condensed phases, where traditional MSs are difficult to introduce, and usually extend to infinity in isolated systems, where it is theoretically arbitrary to define the exterior limit of an atom or molecule. Since IASs are uniquely associated to a pair of bonded atoms, every AIMMS in a condensed phase system may be partitioned into as many polygonal faces[11] as the coordination index of its inner nucleus. AIMMSs are thus homeomorphic to polyhedra. In the process of construction of the AIMMS, only the intermolecular IASs, i.e., those coming from intermolecular bonds, get exposed to the exterior envelope and contribute to the AIMMS.

The significance of the quantum mechanical MSs comes not only from their neat theoretical origin, but also from being faceted entities that gather a wealth of quantitative information about intermolecular interactions. In particular, knowledge of the reduced density matrices at the points belonging to the AIMMS allows us to obtain the most important energetic and force-related quantities of a molecule. It is possible to show[22] that the first and second order density matrices define the microscopic stress tensor, $\boldsymbol{\sigma}(\vec{r})$. The surface integral of $\boldsymbol{\sigma}$ over the AIMMS gives the total force exerted by the surroundings on the molecule under study. It vanishes at equilibrium, and it may be decomposed into intermolecular contributions. For example, if S_{AB} is the face of our AIMMS that corresponds to the intermolecular bond between the atoms *A* (belonging to our molecule) and *B* (from the surroundings),

$$\vec{F}_{AB}=\oint_{S_{AB}}\boldsymbol{\sigma}\cdot d\vec{S}, \tag{2}$$

is the action–reaction total force that these bonded atoms exert on each other. Furthermore, using similar expressions one has access to the total energy of the molecule and its decomposition into kinetic and potential contributions, or to the pressure exerted by the environment on the molecule. These magnitudes, together with the values of the electron density and its Laplacian at the intermolecular bcp, which are necessarily found onto the AIMMS, characterize quantitatively the intermolecular interactions.

Fortunately, if only a qualitative picture of the interactions is needed, then it is known[18] that the shape and curvature of the IASs faithfully reflect some of the previous magnitudes. The Gaussian curvature of an IAS at a bcp is related to the third derivatives of the electron density and, therefore, to the Ehrenfest forces acting among the electrons of the bonded quantum subsystems. Planar faces are found in interactions with no detectable charge transfers, like in symmetric homoatomic bonds, whereas curved faces indicate non-negligible charge transfer and subsequent polarization of the electron density. It is invariably found that if atom *A* donates charge to atom *B* upon bonding, the IAS is curved towards *A*, the cationic species. Thus cations tend to adopt convex spherical shapes, while anions acquire concave excavations along cation–anion directions, at least in the vicinities of bond critical points. Actually, the final curvature of an IAS is found to be a measure of the *hardness*, or deformability, of the bonded atoms. Highly polarizing cations, like Li^+, give rise to very curved surfaces when bonded to very polarizable anions, like I^-. A quick look at the shape of an AIMMS in a solid, for instance, gives an intuitive, yet rigorous picture of

the type, intensity, and location of the various intermolecular interactions existing among its constituent molecules.

Despite the firm theoretical background that supports the use of AIMMSs, their computation is far from easy. The absence of an algebraic condition for locating points situated onto the IASs has been long recognized as the source of this difficulty. Several algorithms have been proposed over the years[23–25] to improve the robust, but extremely slow, bipartition technique. Though the computational efficiency of these methods is much greater than that of the original proposals, obtaining accurate IASs is still a time consuming computational task. Simple, easy to compute approximations to AIMMSs that keep the basic shape of the surfaces are necessary in order to spread their use, yet maintaining as close as possible a relationship to rigorously defined entities. WPPs, which are good zero order approximations to IASs if topological radii are chosen to remove their arbitrariness, are however not suited for this purpose, for all their faces are strictly planar and do not convey information about interactions.

Spackman and Byrom[13] have devised a simple method to obtain well-defined molecular surfaces based on the Hirshfeld stockholder partitioning[14] of the electron density. Hirshfeld partitioning divides any scalar density into atomic or molecular contributions with respect to a reference value of the scalar in the isolated atom or molecule. Usually, the spherically averaged atomic densities coming from Clementi and Roetti's near Hartree–Fock atomic wave functions[26] are used to build the reference, giving rise to the so-called promolecular or procrystalline densities,

$$\rho_{\text{promolecule}} = \sum_{A \in \text{molecule}} \rho_A ,$$
$$\rho_{\text{procrystal}} = \sum_{A \in \text{crystal}} \rho_A , \tag{3}$$

where ρ_A is the Clementi and Roetti's density of atom A. This is a very convenient recipe, but many other references can be used. One can now isolate a given constituent S in the system (an atom or group of atoms in a molecule, a molecule in a crystal, etc.) and define its Hirshfeld weight function, $w_S(\vec{r})$ as

$$w_S(\vec{r}) = \frac{\Sigma_{A \in S} \rho_A(\vec{r})}{\rho(\vec{r})}, \tag{4}$$

where ρ is the promolecular or procrystalline density. The Hirshfeld surface of S is now defined as the geometrical locus of points satisfying $w_S = 0.5$. Since HSs may be seen as special isosurfaces of the w weight function, there exist very efficient algorithms to obtain and display them in a computationally inexpensive way.

As Spackman and Byrom showed in their paper, HS partitioning is uniquely defined, and HS basins do not overlap, filling the space almost completely. The empty space left by the HS basins are found in regions of very low electron density and usually account for less than about 5% of the total volume. As commented in the introduction, these surfaces are strikingly similar to AIMMSs, but the reasons behind this behavior are poorly understood. As we will show in the following, there are a number of reasons that justify the similarity between both kinds of surfaces.

III. THE EXPONENTIAL MODEL

Our approach is based, in the first place, on substituting the exact electron density by its promolecular or procrystalline analogue. The latter is known to have the same topology as the exact density in most meaningful cases. In the second place, we model the density in the interstitial regions that harbor potential loci for the AIMMSs/HSs by the sum of exponentially decreasing contributions centered at the neighboring nuclei. This is the exponential tail model.[18] It has been shown to provide a simple way to rationalize many correlations found on examining the topology of the theoretical electron density when studying families of related crystalline compounds. In order to simplify the discussion, we will restrict it to a two atom model, but the results are easily extrapolated to general situations.

Let us consider two nuclei A and B separated by a distance r_{ab}, and two spherical exponentially decreasing densities centered on them. The total density may be written as

$$\rho(\vec{r}) = \rho_A + \rho_B = a e^{-\alpha r_a} + b e^{-\beta r_b}, \tag{5}$$

where r_a and r_b are the distances from point $\vec{r}$ to centers A and B, respectively. In this model, a and b scale with the nuclear charge, and α and β capture the size extension of the atomic densities. It is easy to show[18] that, for reasonable values of the parameters, this model has a bcp located on the internuclear axis at a distance measured from the A center equal to

$$r_a^{\text{bcp}} = \frac{1}{\alpha+\beta}\left(\ln\frac{a\alpha}{b\beta} + \beta r_{ab} \right). \tag{6}$$

The HS separating both atoms can also be constructed analytically. The Hirshfeld weight function isosurfaces $w_A(\vec{r}) = k$ satisfy the relation

$$\alpha r_a - \beta r_b = \ln\left(\epsilon \frac{a}{b} \right), \quad \epsilon = \frac{1}{k} - 1. \tag{7}$$

The Hirshfeld surface is simply obtained by choosing $k = 1/2$. The families of surfaces described by Eq. (7) are hyperbolic sheets that may be easily examined with any computational algebra code. They are actually biparametric, $r_a - \lambda r_b = \mu$, with $\lambda = \beta/\alpha$, and $\mu = \alpha^{-1} \ln(\epsilon a b^{-1})$, so all the possible isosurfaces coming from the model can be studied in this λ, μ space. Except the $\lambda = 1$ case, in which the isosurfaces are unbounded hyperboloids with foci at the nuclear positions, the rest of the cases give rise to closed revolution surfaces.

Figure 1 displays the HSs of this model both at fixed a/b ratio and variable λ and at fixed λ and variable a/b. Decreasing λ, which in this model corresponds to compacting the ρ_A component of the density with respect to the ρ_B one, shrinks the size of the A atom and increases the curvature of the HS surface. Decreasing μ has a similar effect. This latter case may be linked to either an increase of the isosurface value k (everything else constant), or to a decrease of the

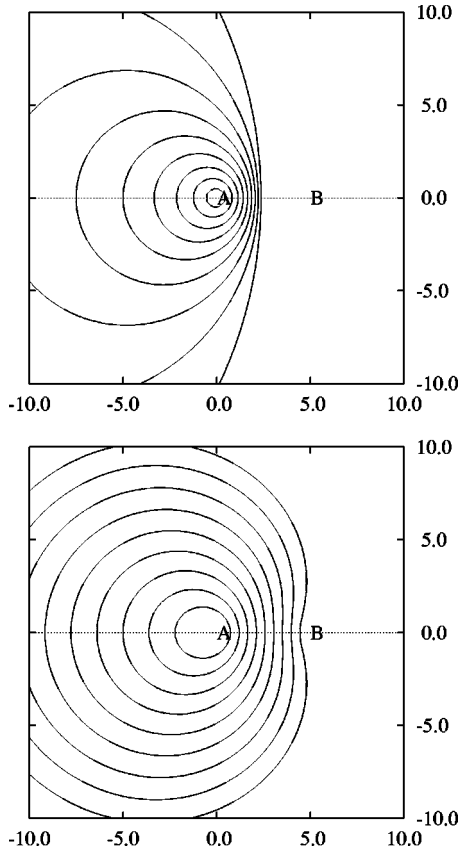

FIG. 1. $r_a-\lambda r_b=\mu$ isosurfaces for the two atom model discussed in the text. Nuclei A and B are placed on the x axis at $x=0$, and $x=5.0$, respectively. On the upper figure, $\epsilon=a=b=\alpha=1$, and β changes linearly from $\beta=0.1$ (isosurface closest to A) to $\beta=0.9$. On the lower, $\epsilon=a=1$, $2\beta=\alpha=1$, and $b=4\times2^{-n}$, with n varying linearly from $n=0$ (isosurface closest to A) to $n=8$. All units are arbitrary.

atomic number of A with respect to that of B. When actual systems are modeled this way,[18] it is difficult to find λ values greater than about 3–4, and a/b ratios greater than 30–40. This means that for all the physically reasonable values of the parameters, the most compact atom is that with a convex HS, the more compact the density, the more curved the surface. This is exactly the behavior shown by Spackman and Byrom in a number of crystals.[15,16]

The intersection of the Hirshfeld weight function isosurfaces with the internuclear axis are easily found from Eq. (7) to be

$$r_a^{\mathrm{int}}=\frac{1}{\alpha+\beta}\left(\ln\frac{a\epsilon}{b}+\beta r_{ab}\right), \tag{8}$$

so the bcp coincides with the intersection of the w isosurface corresponding to $\epsilon=\alpha/\beta$ or $k=\beta/(\alpha+\beta)$ with the internuclear axis. Such an isosurface has very interesting properties. It coincides with, and is tangent to the IAS at the bcp, as both surfaces are revolution surfaces around the internuclear axis, and most importantly, it has approximately the same curvature as the IAS. It is also easy to examine the properties of this particular isosurface with respect to the $\vec{\nabla}\rho$ field that defines the IAS. All points onto this isosurface satisfy the following two equations, obtained by differentiating Eqs. (5) and (7),

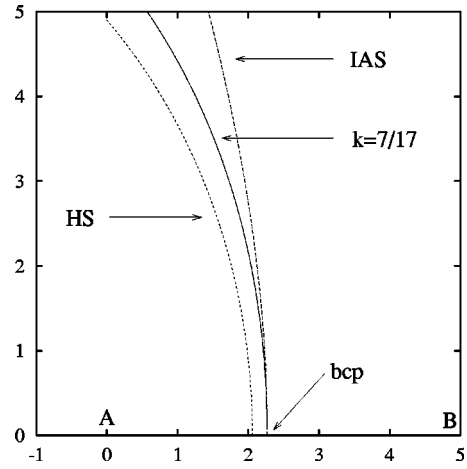

FIG. 2. Comparison among the HS, the IAS, and the $w=\beta/(\alpha+\beta)$ isosurface for the two atom model with $a=b=\alpha=1$, $\beta=0.7$, $r_{ab}=5$. Only a semiplane is shown. All labeling is the same as Fig. 1.

$$\begin{aligned}&\vec{\nabla}\rho(\vec{r})=-a\alpha e^{-\alpha r_a}(\vec{u}_a+\vec{u}_b),\\&(\alpha\vec{u}_a-\beta\vec{u}_b)\cdot d\vec{r}=0.\end{aligned} \tag{9}$$

In these expressions, $\vec{u}_a$ and $\vec{u}_b$ are unitary vectors along the $\vec{r}_a$ and $\vec{r}_b$ directions, respectively. The tangent vector of the w isosurface at any of its points is orthogonal to the $\alpha\vec{u}_a-\beta\vec{u}_b$ vector, while the flux line of the density gradient that crosses that point is parallel to the $\vec{u}_a+\vec{u}_b$ vector. If both vectors are orthogonal at any point, the flux line will be contained in the w isosurface. This is approximately satisfied when α and β do not differ much, which makes the condition for the w isosurface a good approximation for the IAS.

The $w=0.5$ isosurface, or HS, does not pass exactly through the bond point, but is displaced with respect to it by the quantity

$$\Delta=r_a^{\mathrm{bcp}}-r_a^{\mathrm{int}}(\mathrm{HS})=\frac{1}{\alpha+\beta}\ln\frac{\alpha}{\beta}, \tag{10}$$

that depends only on the exponents of the atomic densities. In the systems explored so far, the alkali halides,[18] where very compact cations face to large, diffuse anions, α and β span a rather limited range, from about 1.5 to 6 a.u. For example, the LiI crystal, with a small lithium cation (topological radius close to 1.7 bohr) and a very large iodine anion (radius around 4.1 bohr) has $\alpha=5.64$, $\beta=1.96$ a.u. Δ is then usually quite small, around tenths of a bohr, and often smaller than 0.1 bohr. Most other interactions that may be simulated by the exponential model will involve atomic species with even more similar decaying exponents. Taking into account the smooth variation of the w isosurfaces on changing ϵ (as it is shown by Fig. 1), and the arguments of the previous paragraphs, we can definitely state that in the neighborhood of a bcp, HSs and IASs are very similar in both location and shape.

We are now in a position to compare the general properties presented above with actual numerical results. Figure 2 shows the $k=\beta/(\alpha+\beta)$ isosurface, the HS, and the IAS for a particular choice of the parameters of the model ($a=b$

$=\alpha=1$, $\beta=0.7$, $r_{ab}=5$). We can check how the HS is a very good approximation to the IAS up to about 3 bohr away from the bcp in the perpendicular direction to the internuclear axis.

When many centers are present, the AIMMS will be the union of several IASs, each of them corresponding to a different bcp (intermolecular interaction). Near those bcp's, the density will be very accurately represented by a two-atom model, with atomic densities coming from the bonded nuclei. As distances between different bcp's cluster around a few bohr, the molecular HS will display discernible faces in a one to one correspondence with those of the AIMMS. The similarity of both surfaces will be greatest near the bcp's, precisely the regions of greatest interest. In summary, as far as the interatomic/intermolecular interactions present in a given system may be adequately described by the exponential model and the decaying rate of the model densities is not very dissimilar, we should expect a very good fitting among HSs and AIMMs. In those circumstances HSs might then be used as inexpensive alternatives to AIMMSs in qualitative investigations. As a gross rule, strongly polar intramolecular covalent bonds should be bad examples of the above ideas, as the electron density reorganization in the internuclear regions is not easy to model by exponential contributions. On the other hand, any weak intermolecular interaction, ionic bond, or slightly polar covalent system should display similar Hirshfeld and AIM surfaces.

IV. EXAMPLES AND CONCLUSIONS

We have chosen two crystals to illustrate the actual performance of the ideas here presented: LiF in the rock-salt phase, characterized by strong closed-shell ioniclike interactions; and CS_2 in the Cmca phase, a molecular compound with strongly polar shared-shell intramolecular bonds and weak intermolecular closed-shell interactions.

The IASs of the simple ionic alkali halides are known.[18] In most cases there appear cation–anion bcp's along the first neighbor directions and anion–anion bcp's along the second neighbor directions. Thus the cation displays six bonds (and its atomic surface displays six faces) and the anion $6+12$ bonds. The anion–anion contact faces are planar, but the cation–anion surfaces are usually quite curved. These are neat examples of how charge transfer affects the curvature of the surfaces. If there is no charge transfer, like in the symmetric anion–anion faces, the IASs remain planar. If one of the bonded species donates charge to its counterpart, their common IAS becomes curved, getting convex for the cation and concave for the anion. It is also usual that the IASs of cations display odd features like spikes or winglike protrusions. The origin of these entities has been traced back to the fulfillment of certain topological requirements[11] which, very succinctly, are related to the relative size of anions and cations. Spikes, for instance, are formed if the cationic to anionic size ratio is smaller than, but close to 1. In these cases a spike is easier to form than a new edge in a face, which would involve the unfolding of two new critical points of the ring and cage type, respectively.

We have used the multi-ζ, near Hartree–Fock wave functions of Clementi and Roetti[26] to construct the procrystalline density of the LiF crystal in its rock-salt phase (space group $Fm\bar{3}m$) at the experimental lattice parameter, $a=3.904$ Å. A simple adaptation of our CRITIC code[11] has been employed to obtain both the IASs and the HSs in the system, and to integrate some interesting functionals over them.

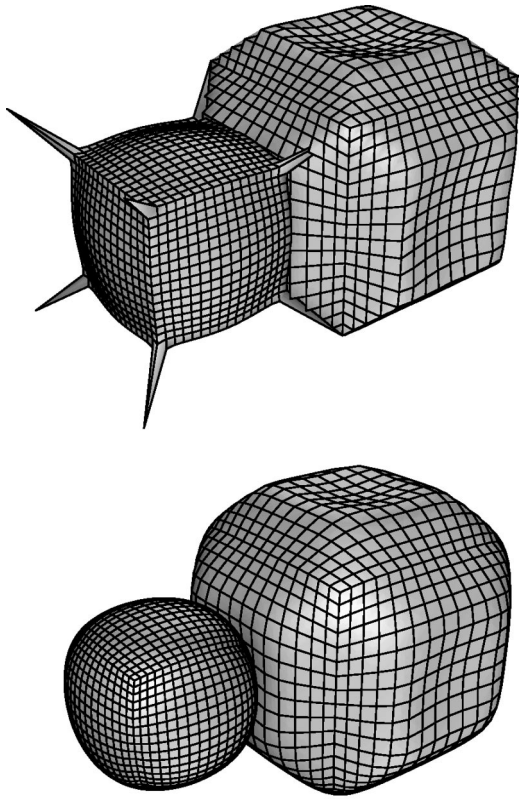

FIG. 3. Interatomic (top) and Hirshfeld (bottom) surfaces in the rock-salt phase of the LiF crystal at the experimental geometry, $a=3.904$ Å. In each picture only a Li^+ cation (small object) and an adjacent F^- anion (large object) are shown. Views and scales are common.

The shapes of the surfaces are shown in Fig. 3. Their similarity is apparent. Looking at the IASs, our previous comments become clear, and the six spiked faces of the Li^+ ion and the $6+12$ face of the anion are easily recognized. All the critical points of the electron density are located on the IASs. In our case, the Li–F bcp is at the middle of the square faces, and the F–F bcp is at the geometrical center of the 12 hexagonal faces. The ring points are found at the center of the edges of the square faces, and the cage points (local minima) at the confluence of three hexagonal faces shown in the pictures, onto a C_{3v} axis. These are the only real vertices of our polyhedra, and the origin of the spikes as previously reported.

The topological faces of the IASs remain practically unmodified in the HSs, and the polyhedral nature of the ions is still easily recovered. As the anion is regarded, the 12 planar F–F contacts remain mostly planar in the HS of the fluoride, though the sharpness of the edges of the faces has been smeared out. On the other hand, the six concave Li–F faces remain concave, though the curvature at the bcp is slightly smaller in the HS. The shape of the HS of the Li^+ cation follows the same trends, and though in a first look it seems

TABLE I. Formal charges and volumes of the Li^+ and F^- ions as obtained by integration over the Hirshfeld and interatomic surfaces. All data in atomic units.

	Li^+	F^-
Q(IAS)	+0.948	−0.948
Q(HS)	+0.994	−0.924
V(IAS)	16.97	83.43
V(HS)	11.80	81.03

rather spherical, a closer inspection reveals a clear cubelike geometry. It is important to notice that the ionic basins fill the space completely, and that this means that the cations fit perfectly into the holes left by the anionic stacking. This is not the case for the HSs, and the empty spaces are easily seen in the figure. HSs usually lack the complexity that this requirement imposes on the IASs, but as we can see, they maintain most of their qualitative features.

It is also interesting to compare some quantitative characteristics of the ions defined by these surfaces. We have integrated the charge density and the unit operator to obtain the total formal charges and volumes of the ions, respectively. The results are shown in Table I. As sizes are regarded, it is clear that the ions defined by the HSs are smaller than the quantum subsystems. This fact is clear from the inspection of Fig. 3. The HS cation is 30% smaller than the AIM one. However, this figure decreases to just 3% in the fluoride. As the cation is much smaller than the anion, in the end, only a 7.5% of the volume per LiF unit is lost. The volume not accounted for by the HS ions has a very low electron density. This is seen from the charge partition. Only 0.07 electrons per LiF unit reside in the empty spaces. Since the AIM charge of ions in these highly ionic compounds is always close to nominal, and the HS cation is smaller than the topological one, the number of electrons within the Li^+ HS turns out to be very close to that of a two electrons $1s^2$ core.

CS_2 crystallizes at low temperature in a Cmca structure. At 138 K, its lattice constants are $a=6.312$ Å, $b=5.498$ Å, $c=9.020$.[27] We have computed its Hartree–Fock electronic structure by means of the CRYSTAL package,[28] using double-ζ quality basis sets with d polarization functions and optimized diffuse exponents at both the C and S atoms. The Clementi and Roetti[26] functions for the ground state Russell–Saunders multiplets of the carbon and sulfur atoms have been used to obtain procrystalline and promolecular densities. The same version of the CRITIC code commented above has provided the IASs and HSs of the system.

Two kinds of surfaces may be constructed for such a system, depending on the particular partitioning into constituents chosen [see Eq. (4)]. We may focus our attention on the atoms, and obtain the surfaces for the carbon and sulfur species, or on the molecules, and get the CS_2 molecular surface. As the interatomic surfaces are regarded, the C and S IASs may be perfectly glued into the CS_2 AIMMS. This does not hold for the HSs. Figure 4 shows all these surfaces projected on a (001) plane of the crystal, together with some isocurves of the electron density that help isolate the individual molecules and atomic cores. Six particular CS_2 molecules sitting on the plane, and labeled alphabetically from A to F, have been distinguished. On all of them the IASs (AIMMSs) have been depicted as thick full lines that clearly tesselate the plane. HSs are shown as dashed lines. Mol-

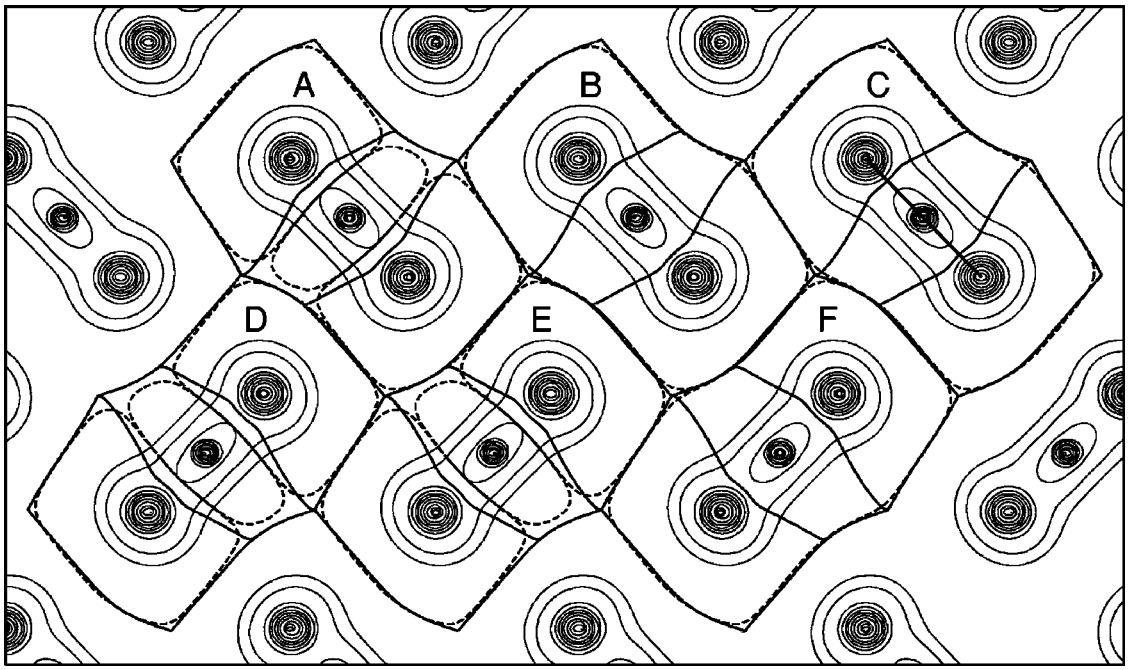

FIG. 4. Molecular surfaces of the Cmca phase of the CS_2 crystal at the experimental geometry projected onto the (001) plane. Six molecules, labeled from A to F, have been selected to display HSs and IASs. Isolines of the electron density with $\rho=0.016\times 2^n$ a.u., $n=0,1,\ldots,10$, are also shown to help locate the atomic positions. The internuclear S–C–S axis is shown in molecule C. Thick full lines represent IASs (AIMMSs), while thick dashed lines depict atomic (in molecules A, D, and E) or molecular (in molecules B, C, and F) HSs. See the text for more details.

ecules A, D, and E show the atomic HSs, while molecules B, C, and F display the molecular HSs.

The coexistence of both strong and weak bonds in these molecular crystals beautifully illustrates some of our ideas. On the one hand, the AIMMSs show the crystal packing effects and the intermolecular interactions quite neatly. The intramolecular carbon–sulphur surfaces are among a well-known class of difficult IASs (that also includes the C–O double and triple bonds) characterized by a change in the sign of their curvatures as we depart from the bond critical point (see molecule C to easily locate bond points). This is due to a rather strong density reorganization in the internuclear region upon bond formation, that at the least seems difficult to simulate with our exponential model. In this sense, the atomic HSs depicted in molecules A, D, and E, show that the carbon–sulphur contact is not very well mimicked. Actually, if the C–S IAS did not display the curvature change, the atomic HSs would be much better approximations to it. The void regions left by the atomic HS partitioning are best viewed near the contact region among the A, D, and E molecules. As in our previous example, they account for about 7% of the total cell volume.

The molecular HSs in molecules B, C, and F are extraordinarily good approximations to the AIMMSs, deviations being noticeable only in the neighborhood of the cusp points of the latter. Loosely speaking, the molecular HSs seem just smoothed versions of the AIMMSs. Let us notice, once again, that the physically important curvature information stored in the AIMMSs is very well preserved on passing to the molecular HSs, and that the one to one correspondence among IAS and HS faces is patent. Voids now occupy less than 2% of the cell volume.

These facts all emerge from our previous arguments. In particular, the worse than expected performance of the exponential model in the carbon–sulphur surfaces, and the very good match between HSs and AIMMs. The latter is expected in most molecular solids, for intermolecular regions are very well described by the exponential model. Moreover, if the different molecules in such solids are made of atoms with not so different size extension, as measured by our exponents α and β, the molecular HSs will be extremely good approximations to the AIMMSs.

Although many other kinds of systems remain to be explored, the ideas here presented are of rather general validity. We have shown that there is a clear algebraic link between HSs and AIMMSs. We think that the HS concept is an easy to compute, easy to visualize way to approximate AIMMSs, and that it is this property that confers HSs the ability to inform about intermolecular interactions in condensed phases.

ACKNOWLEDGMENTS

The authors are grateful to the Ministerio de Ciencia y Tecnología, Project No. BQU2000-0466, for financial support.

[1] M. L. Connolly, Network Science (1996). www.netsci.org/Science/Compchem/feature14.html
[2] R. B. Corey and L. Pauling, Rev. Sci. Instrum. **24**, 621 (1953).
[3] M. L. Connolly, Science **221**, 709 (1983).
[4] R. F. W. Bader, W. H. Henneker, and P. E. Cade, J. Chem. Phys. **46**, 3341 (1967).
[5] T. S. Koritsanszky and P. Coppens, Chem. Rev. **101**, 1583 (2001).
[6] P. Ordejón, Comput. Mater. Sci. **12**, 157 (1998).
[7] See, for instance the citations section of Ref. 1.
[8] E. Wigner and F. Seitz, Phys. Rev. **43**, 804 (1933).
[9] See any treatise on computational geometry. For instance, *Graphic Gems*, edited by A. S. Gladner (Academic, New York, 1994).
[10] P. Coppens, Phys. Rev. Lett. **35**, 98 (1975).
[11] A. Martín Pendás, A. Costales, and V. Luaña, Phys. Rev. B **55**, 4275 (1997).
[12] R. F. W. Bader, *Atoms in Molecules* (Oxford University Press, Oxford, 1990).
[13] M. A. Spackman and P. G. Byrom, Chem. Phys. Lett. **267**, 215 (1997).
[14] F.L. Hirshfeld, Theor. Chim. Acta **44**, 129 (1977).
[15] J. J. McKinnon, A. S. Mitchell, and M. A. Spackman, Chem.-Eur. J. **4**, 2136 (1998).
[16] J. J. McKinnon, A. S. Mitchell, and M. A. Spackman, Chem. Commun. (Cambridge) **1998**, 2071.
[17] V. Luaña, A. Costales, and A. Martín Pendás, Phys. Rev. B **55**, 4285 (1997).
[18] A. Martín Pendás, A. Costales, and V. Luaña, J. Phys. Chem. B **102**, 6937 (1998).
[19] J. Schwinger, Phys. Rev. **82**, 914 (1951).
[20] M. A. Blanco, A. Costales, A. Martín Pendás, and V. Luaña, Phys. Rev. B **62**, 12028 (2000).
[21] M. E. Eberhart, M. M. Donovan, and R. A. Outlaw, Phys. Rev. B **46**, 12744 (1992).
[22] O. H. Nielsen and R. M. Martin, Phys. Rev. B **32**, 3780 (1985).
[23] F. W. Biegler-König, T. T. Nguyeng-Dang, Y. Tal, R. F. W. Bader, and A. J. Duke, J. Phys. B **14**, 2739 (1981).
[24] P. L. A. Popelier, Theor. Chim. Acta **87**, 465 (1994).
[25] J. Cioslowski and B. Stefanov, Mol. Phys. **84**, 707 (1995).
[26] E. Clementi and C. Roetti, At. Data Nucl. Data Tables **14**, 177 (1974).
[27] N. C. Baenziger and W. L. Duax, J. Chem. Phys. **48**, 2974 (1968).
[28] R. Dovesi, V. R. Saunders, C. Roetti, M. Causà, N. M. Harrison, and R. Orlando, CRYSTAL98, User's manual (1999). www.chimifm.unito.it/teorica/crystal/crystal.html